BBA - Molecular Basis of Disease 1865 (2019) 2441–2450

Contents lists available at ScienceDirect

BBA - Molecular Basis of Disease

journal homepage: www.elsevier.com/locate/bbadis

The Smad3-miR-29b/miR-29c axis mediates the protective effect of macrophage migration inhibitory factor against cardiac fibrosis

Jing-nan Liang[a,b,c,1], Xiao Zou[a,b,1], Xian-hong Fang[a,1], Jin-dong Xu[d], Zhen Xiao[a,b], Jie-ning Zhu[a,b], Hui Li[c], Jing Yang[e], Ni Zeng[e], Shu-jing Yuan[e], Rong Pan[f], Yong-heng Fu[a,b], Ming Zhang[b], Jian-fang Luo[b], Sheng Wang[d], Zhi-xin Shan[a,b,*]

[a] Guangdong Provincial Key Laboratory of Clinical Pharmacology, Guangdong Cardiovascular Institute, Guangzhou 510080, China
[b] Research Center of Medical Sciences, Guangdong Provincial People's Hospital, Guangdong Academy of Medical Sciences, Guangzhou 510080, China
[c] School of Pharmacology, Southern Medical University, Guangzhou 510515, China
[d] Department of Anesthesiology, Guangdong Cardiovascular Institute, Guangzhou 510080, China
[e] School of Medicine, South China University of Technology, Guangzhou 510632, China
[f] School of Biology and Biological Engineering, South China University of Technology, Guangzhou 510632, China

ARTICLE INFO

Keywords:
Macrophage migration inhibitory factor
Cardiac fibrosis
MicroRNA-29b-3p
MicroRNA-29c-3p
Smad3

ABSTRACT

Although macrophage migration inhibitory factor (MIF) is known to have antioxidant property, the role of MIF in cardiac fibrosis has not been well understood. We found that MIF was markedly increased in angiotension II (Ang-II)-infused mouse myocardium. Myocardial function was impaired and cardiac fibrosis was aggravated in *Mif*-knockout (*Mif*-KO) mice. Functionally, overexpression of MIF and MIF protein could inhibit the expression of fibrosis-associated collagen (Col) 1a1, COL3A1 and α-SMA, and Smad3 activation in mouse cardiac fibroblasts (CFs). Consistently, MIF deficiency could exacerbate the expression of COL1A1, COL3A1 and α-SMA, and Smad3 activation in Ang-II-treated CFs. Interestingly, microRNA-29b-3p (miR-29b-3p) and microRNA-29c-3p (miR-29c-3p) were down-regulated in the myocardium of Ang-II-infused *Mif*-KO mice but upregulated in CFs with MIF overexpression or by treatment with MIF protein. MiR-29b-3p and miR-29c-3p could suppress the expression of COL1A1, COL3A1 and α-SMA in CFs through targeting the pro-fibrosis genes of transforming growth factor beta-2 (*Tgfb2*) and matrix metallopeptidase 2 (*Mmp2*). We further demonstrated that Mif inhibited reactive oxygen species (ROS) generation and Smad3 activation, and rescued the decrease of miR-29b-3p and miR-29c-3p in Ang-II-treated CFs. Smad3 inhibitors, SIS3 and Naringenin, and *Smad3* siRNA could reverse the decrease of miR-29b-3p and miR-29c-3p in Ang-II-treated CFs. Taken together, our data demonstrated that the Smad3-miR-29b/miR-29c axis mediates the inhibitory effect of macrophage migration inhibitory factor on cardiac fibrosis.

1. Introduction

Cardiac fibrosis participates in many cardiac pathophysiologic processes, with the characterizations of proliferation of cardiac fibroblasts and excessive accumulation of the extracellular matrix (ECM) in the myocardium [1]. Meanwhile, changes in fibrillar collagen synthesis and degradation, as well as changes in the degree of collagen cross-linking occur in the ECM during the process of myocardial fibrosis. The initial reparative fibrosis is crucial for preventing rupture of the ventricular wall, however, the exaggerated fibrotic response contributes to progressive impairment of cardiac function, heart failure, fatal arrhythmia and sudden cardiac arrest [2]. Understanding the mechanisms responsible for cardiac fibrosis is crucial to develop anti-fibrotic therapy strategies in the clinic.

Macrophage migration inhibitory factor (MIF) is a cytokine with oxidoreductase activity [3,4]. MIF plays important roles in inflammatory diseases, such as sepsis [5], rheumatoid arthritis [6,7], obesity [8] and atherosclerosis [9,10]. Increasing evidence shows that MIF plays important roles in cardiac homeostasis and regulation of cardiac function under pathological conditions, including diabetes mellitus [11,12], myocardial infarction [13], ischemia-reperfusion injury [14,15], pressure overload-induced cardiac hypertrophy [16,17] and doxorubicin-induced cardiac anomalies [18]. MIF deficiency exacerbates aging-induced myocardial fibrosis in mice [19]. However, the

* Corresponding author at: Room 1107, Weilun Bldg, 96 Dongchuan Road, Guangzhou 510080, Guangdong, China.
E-mail address: shanzhixin@gdph.org.cn (Z.-x. Shan).
[1] These authors contributed equally to this work.

https://doi.org/10.1016/j.bbadis.2019.06.004
Received 22 January 2019; Received in revised form 15 May 2019; Accepted 3 June 2019
Available online 06 June 2019

precise mechanism underlying the anti-fibrosis effect of MIF remains elusive.

MicroRNAs (miRNAs) are endogenous, non-coding, and 20–23 nucleotide RNAs that negatively regulate a variety of target genes, such as those genes involved in cardiovascular diseases [20,21]. Recent studies have demonstrated that miRNAs are implicated in the myocardial fibrosis; for example, miR-21, -29, -30, -133, -214, -433 and -590 modulate the expression of fibrosis-related genes in animal models of ischemia/reperfusion myocardial infarction, trans-aortic constriction, angiotension (Ang)-II infusion-induced myocardial fibrosis, nicotine-induced atrial fibrosis, respectively [22–24]. However, it remains unknown whether miRNAs mediate the effect of MIF in cardiac fibrosis.

In the present study, we determined the expression of MIF in the myocardium of Ang-II-infused mice and Ang-II-induced cardiac fibroblasts (CFs), detected myocardial fibrosis in Ang-II-infused *Mif* knockout (*Mif*-KO) mice and revealed the anti-fibrotic role of MIF in cardiac fibrosis. Furthermore, we showed that MIF inhibited the expression of fibrosis-associated COL1A1, COL3A1 and α-SMA, attenuated Smad3 activation, and up-regulated the expression of miR-29b-3p, -29c-3p in CFs. Our further studies demonstrated that miR-29b-3p and miR-29c-3p inhibited cardiac fibrosis by targeting *Tgfb2* and *Mmp2*, and the Smad3 signaling negatively regulated the expression of miR-29b-3p and miR-29c-3p in CFs. Our results have supported an anti-fibrotic effect of MIF on cardiac fibrosis.

2. Materials and methods

2.1. Ethics statement

Male C57BL/6 mice weighing 20 ± 3 g [License number SCXK (YUE) 2004–0011, Department of Experimental Animal Research Center, Sun Yat-sen University, Guangzhou, China], and male Mif knock-out (Mif-KO, J003830) mice and wide type (WT) control mice weighing 20 ± 3 g [License number SCXK (YUE) 2004–0011, Nanjing Biomedical Research Institute of Nanjing University, Nanjing, China] were used in the current studies. Adult mice were housed in a pathogen-free condition with a 12-h light/dark cycle and free access to standard mouse chow and tap water. This study confirmed to the Guide for the Care and Use of Laboratory Animals published by the US National Institutes of Health (8th Edition, National Research Council, 2011). The present program was also approved by the research ethics committee of Guangdong General Hospital (the approval number: No. GDREC2010093A).

2.2. Animal studies

We established a mouse model of Ang-II (1.46 mg/kg/d, 14 d) infusion-induced cardiac hypertrophy as we previously described [25]. Briefly, mice were anesthetized through the intraperitoneal application of sodium pentobarbital (50 mg/kg), followed by implantation of the Ang-II mini-osmotic pump (alzet model 2002, Cupertino, CA, USA). The adequacy of anesthesia was confirmed by the absence of reflex response to foot squeeze. Body temperature was maintained at 37 ± 0.5 °C during surgery. At the end of the experiments, mice were killed with the intraperitoneal injection of an overdose of sodium pentobarbital (200 mg/kg) after echocardiography, and the myocardial tissue was collected for further detections.

2.3. Echocardiographic study

Left ventricular (LV) function variables were assessed by transthoracic echocardiography. After the induction of light general anesthesia, the rats underwent transthoracic two-dimensional guided M-mode echocardiography with an 8.5-MHz transducer (Acuson, Mountain View, CA). From the cardiac short axis (papillary level), we measured the LV anterior wall end-diastolic thickness (LVAWd), the systolic LV anterior wall thickness (LVAWs), the LV internal dimension at end-diastole (LVIDd), the LV internal dimension at end-systole (LVIDs), the LV posterior wall end-diastolic thickness (LVPWd), the LV posterior wall end-systolic thickness (LVPWs), the ejection fraction (EF) and fractional shortening (FS). Echocardiographic measurements were averaged from at least three separate cardiac cycles.

2.4. Histological analysis

Formalin-fixed mouse or human myocardium specimens were embedded in paraffin and cut into 4 μm thick sections. Tissue sections were mounted on the regular glass slides and stained with 1.0 mg/ml Alexa Fluor® 488 conjugate of wheat germ agglutinin (WGA) solution (Molecular Probes, Eugene, Oregon, USA) to demonstrate the sizes of cardiomyocytes in mouse or human ventricular myocardium. Tissue sections were also stained with Masson's trichrome for histological analyses. To analyze the collagen volume fraction (CVF) in the border zone of the infarcted region, we selected eight separate views (magnification = original × 400) and assessed CVF using the following formula: CVF = collagen area/total area.

2.5. MiRNA microarray

The analysis of miRNA expression was performed on total RNA extracted from a pool of 6 to 8 myocardium of *Mif*-KO mice or WT control mice with and without Ang-II infusion. Microarray procedures and data analyses were performed at Bioassay Laboratory of CapitalBio Corporation (Beijing, China). Briefly, 200 ng of total RNA extracted from myocardium or plasma samples was fluorescently labeled with Cyanine3-pCp using miRNA Complete Labeling and Hyb Kit (Agilent Technologies, Santa Clara, CA, USA). The labeled samples were then concentrated and hybridized with the Hybridization Chamber gasket slides (Agilent, USA). Arrays were scanned on Agilent chip scanner (G2565CA), and image analysis was performed using Agilent Feature Extraction (v10.7) software (Agilent, USA), followed by data normalization using Agilent GeneSpring software (Agilent, USA).

2.6. Isolation, culture and treatment of mouse cardiac fibroblasts (CFs)

Mouse cardiac fibroblasts (CFs) were isolated from cardiac tissues of C57BL/6 mice through digestion with 0.25% trypsin plus 20 IU/ml DNase. CFs were separated from cardiomyocytes by gravity separation and cultured on 10-cm cell culture dishes in growth media (DMEM/LG 10% FBS, 1% penicillin and 1% streptomycin) at 37 °C in humidified air with 5% CO_2. CFs from the third passage were used for the experiments. Transfection of 50 nM miR-29b-3p mimic, miR-29c-3p mimic, miR-29b-3p inhibitor, miR-29c-3p inhibitor, *Mif* siRNA and *CD74* siRNA (RiboBio, Guangzhou, China) was performed using oligofectamine reagent (Invitrogen, Carlsbad, CA, USA). Overexpression of MIF in CFs was achieved by adenovirus vector. In addition, CFs were incubated with DMEM/LG 1% FBS overnight before treatment with 10 mM *N*-acetyl-L-cysteine (NAC, a ROS scavenger; Sigma-Aldrich, St. Louis, MO, USA) or MIF protein (Sino Biological, Beijing, China).

According to our previous report [26], the template DNA of mouse *Mif* gene was directionally inserted into the multiple cloning sites in pAd-Track-CMV vector (Coloncancer, USA), followed by the construction of the recombinant *Mif* adenovirus plasmid and the package of MIF recombinant adenovirus, respectively. Meanwhile, the adenovirus rAd-*Gfp* was prepared as a control vector. CFs were then infected with rAd-*Gfp* and rAd-*Mif* adenovirus (MOI 10), respectively.

2.7. Fluorescence immunohistochemistry (FIHC) assay

Cultured CFs were washed in phosphate-buffered saline (PBS), fixed for 10 min in 3.7% formaldehyde, and permeabilized for 10 min in 0.1% Triton X-100. Monolayers were then washed in blocking solution

and incubated with COL1A1, COL3A1 and α-SMA antibodies (Abcam), respectively, overnight at 4 °C. Monolayers were then rewashed and incubated with Alexa Fluor®555 dye-conjugated IgG (Molecular Probes, Eugene, OR, USA) for 1 h at room temperature. The nuclei were counterstained with 40, 6-diamidino-2-phenylindole (DAPI). Confocal micrographs were obtained using a Leica SP5 confocal microscopy (Leica, Mannheim, Germany). The fluorescence intensity was analyzed using the LAS AF-TCS SP5 imaging software.

2.8. Imaging of DCF fluorescence

Intracellular oxidants in mouse CFs were measured using the probe dichlorofluorescein diacetate (DCFH-DA) and confocal microscopy. In brief, CFs were incubated with 10 μM DCFH-DA for 15 min, followed by washing twice with culture medium and imaging five randomly chosen fields with Leica SP5 Spectral scanning laser confocal microscope (Leica Microsystems, Wetzlar, Germany). The levels of DCF fluorescence were analyzed with Leica Application Suite 2.02 software.

2.9. Quantitative mRNA and miRNA measurements

For detection of mRNA expression of coding genes, first-strand cDNA was generated from 1.5 μg total RNA using a mixture of oligo $(dT)_{15}$ and random primers with superscript reverse transcriptase (Invitrogen, Carlsbad, CA). Quantitative reverse-transcription PCR (RT-qPCR) for miR-29b-3p and -29c-3p was performed on cDNA generated from 0.5 μg total RNA according to the manufacturer's protocol (Ribobio, China). To normalize RNA content, *U6* was used for miRNAs template normalization and *Gapdh* was used for coding gene template normalization. PCR was performed with the ViiA7 Quantitative PCR System (Applied Biosystems, Carlsbad, CA). The $2^{-\Delta\Delta Ct}$ method was used to calculate relative expression levels of the concerned coding genes and miRNAs. PCR primers for miR-29b-3p, -29c-3p, *U6* and coding genes are shown in Supplementary Table 1.

2.10. Western-blot assay

Protein extracts (40 μg) were separated using 12% (wt/vol) SDS-PAGE, transferred onto a polyvinylidene fluoride (PVDF) membrane, and probed with antibodies for α-SMA (Abcam), COL1A1, COL3A1, TGF-β2, MMP2 (Proteintech, Chicago, IL, USA), p-Smad3, Smad3 (Cell Signaling Technology, Beverly, MA, USA), respectively, overnight at 4 °C. Membranes were then washed extensively with TBS/T and incubated with a horseradish peroxidase-conjugated secondary antibody (Santa Cruz) for 1 h at room temperature. Protein was visualized using the ECL Plus detection system (GE Healthcare, WI, USA). For the internal control, the same membranes were also immunoblotted with an anti-GAPDH antibody (Santa Cruz).

2.11. Dual luciferase assay

As shown in our previous report [27], we constructed the recombinant luciferase reporter plasmids containing sequences of potential miR-29b-3p and miR-29c-3p binding sites in 3′ UTR of *Tgfb2* and *Mmp2* genes. Using a site-directed mutagenesis kit (TransGen, Beijing, China), miR-29b-3p and miR-29c-3p complementary binding sequence TGGTGCT was replaced with TGCACGT in the recombinant luciferase reporter plasmids.

Human embryonic kidney (HEK) 293 cells (3×10^5 cells per well in 12-well plate) were co-transfected with 200 ng of recombinant luciferase reporter plasmid, 50 nM miR-29b-3p and miR-29c-3p mimic, and 20 ng of pRL-TK as an internal control (Promega, Madison, WI). Activities of firefly luciferase (FL) and renilla luciferase (RL) were measured 24 h after transfection, and the relative ratio of the FL/RL was used to indicate the knockdown of *Tgfb2* and *Mmp2* by miR-29b-3p and -29c-3p, respectively.

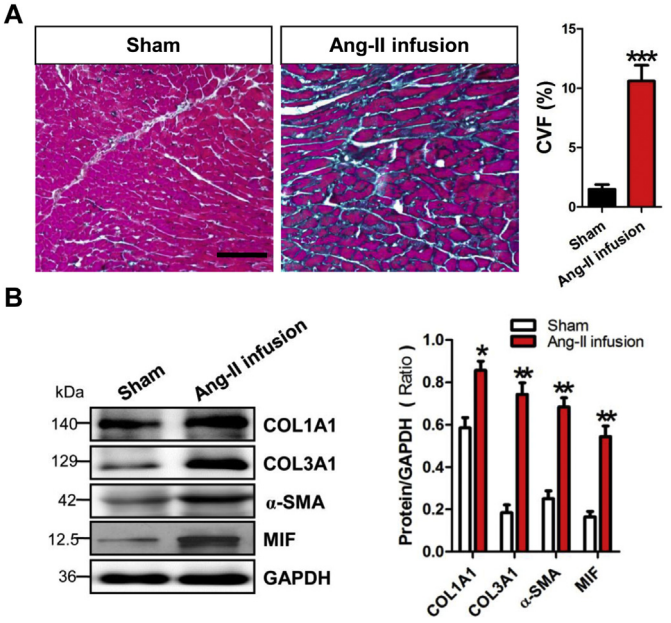

Fig. 1. MIF is upregulated in the fibrotic myocardium of Ang-II-infused mice. (A) Masson's trichrome staining of myocardium of Ang-II infusion mice. Data are shown as the mean ± SEM ($n = 5$). (B) The expression of COL1A1, COL3A1, α-SMA and MIF in the myocardium of Ang-II-infused mice by Western blot assay. Data are shown as the mean ± SEM ($n = 5$). *, $P < 0.05$, **, $P < 0.01$, ***, $P < 0.001$ vs. Sham group.

2.12. Statistical analysis

In each experiment, all determinations were performed at least in triplicate. For analysis of differences between two groups, student's *t*-test was performed. One-way ANOVA followed by Post hoc test (Bonferroni) was chosen for the comparisons of interest without adjustment for multiple comparisons. A value of $P < 0.05$ was considered to be significant. Data were presented as the mean ± the standard error of the mean (SEM). Analyses were performed in IBM SPSS Statistics 25 software.

3. Results

3.1. MIF is upregulated in mouse fibrotic myocardium

Masson's trichrome staining showed that cardiac fibrosis was significantly increased in the myocardium of Ang-II-infused mice (Fig. 1A). Western blot results showed that the expression of fibrosis-related genes, including *Col1a1*, *Col3a1 and Acta2*, was significantly increased in mouse fibrotic myocardium. Meanwhile, MIF expression was also markedly elevated in mouse fibrotic myocardium (Fig. 1B).

3.2. MIF deficiency exacerbates Ang-II-induced cardiac fibrosis in mice

A mouse model of 2-week Ang-II infusion-induced cardiac hypertrophy was established. Echocardiography revealed cardiac structure and function changes in Ang-II-infused *Mif*-KO as compared with WT control mice. Significant decreases in the LV internal diameters (LVIDd, LVIDs) were observed in Ang-II infused *Mif*-KO mice, without significant changes of the LV walls (LVPWd, LVPWs). The ejection fraction (EF) and fractional shortening (FS) were also markedly decreased in Ang-II-infused *Mif*-KO mice (Fig. 2A). Cardiac hypertrophy was further confirmed by the ratio of heart weight to tibial length (Fig. 2B). The Masson's trichrome staining revealed that myocardial fibrosis was markedly increased in Ang-II-infused *Mif*-KO mice (Fig. 2C). Consistently, Western blot results demonstrated that the expression of

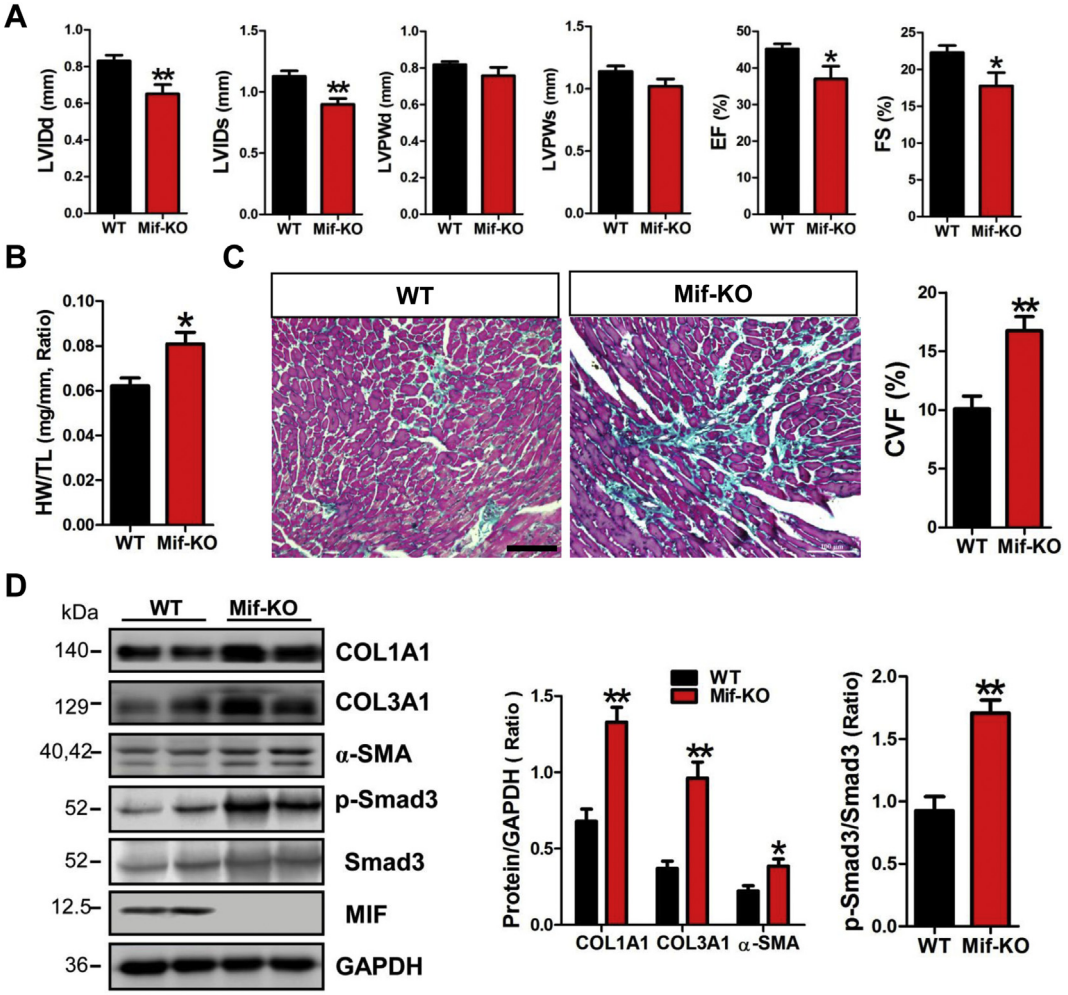

Fig. 2. Cardiac fibrosis is exacerbated in *Mif*-KO mice. (A) Assessment of mouse cardiac function by echocardiography. Data are shown as the mean ± SEM (n = 6–7). (B) The ratio of heart weight to tibial length. Data are shown as the mean ± SEM (n = 6). (C) Masson trichrome staining. The scale bar is 100 μm. Data are shown as the mean ± SEM (n = 6). (D) Protein expression of fibrosis-associated genes, MIF and p-Smad3 level in the myocardium of Ang-II-infused mice by western blot assay. Data are shown as the mean ± SEM (n = 4). *, $P < 0.05$, **, $P < 0.01$ vs. WT group.

COL1A1, COL3A1, α-SMA and the phosphorylated Smad3 (p-Smad3) was significantly increased in the myocardium of Ang-II-infused *Mif*-KO mice (Fig. 2D). Moreover, the colorimetric assay showed that the abilities of hydroxyl radical-scavenging and superoxide anion radical-scavenging in the myocardium of Ang-II-infused *Mif*-KO mice were markedly decreased (Supplementary Fig. 1).

3.3. Effect of MIF on the expression of COL1A1, COL3A1 and α-SMA in CFs

We enhanced the endogenous MIF expression to investigate the effect of MIF on the expression of fibrosis-related genes in mouse CFs. Significant increases in COL1A1, COL3A1 and α-SMA expression were observed in Ang-II-treated CFs, but could be reversed by adenovirus-mediated overexpression of MIF. Consistently, the p-Smad3 level was also efficiently attenuated in Ang-II-treated CFs with MIF overexpression (Fig. 3A).

Then, we inhibited the endogenous MIF expression by *Mif* siRNA in mouse CFs with or without Ang-II treatment. Western blot results showed that expression of COL1A1, COL3A1 and α-SMA was significantly increased in CFs with *Mif* knockdown, and *Mif* knockdown could aggravate Ang-II-induced increase in COL1A1, COL3A1 expression in CFs and also increased p-Smad3 levels (Fig. 3B).

We further blocked the function of the endogenous MIF by MIF inhibitor ISO-1 in mouse CFs treated with Ang-II. Western blot results showed that 10 μM ISO-1 could significantly increase COL3A1 expression, and 30 μM ISO-1 could markedly enhance the expression of COL1A1, COL3A1 and α-SMA. Meanwhile, 30 μM ISO-1 could further enhance Ang-II-induced Smad3 activation in CFs (Fig. 3C).

3.4. MIF protein suppresses COL1A1, COL3A1 and α-SMA expression in mouse CFs

To investigate the effect of exogenous MIF on fibrosis-related gene expression in CFs, MIF protein was used to treat mouse CFs. The results of FIHC assay revealed that the expression of COL1A1, COL3A1 and α-SMA was significantly depressed in mouse CFs treated with 50 ng/ml MIF protein (Fig. 4A). Western blot results confirmed that the expression of COL1A1, COL3A1 and α-SMA was markedly inhibited in CFs by treatment with 50 and 75 ng/ml MIF, respectively (Fig. 4B). Meanwhile, the knockdown of MIF receptor *CD74* could abolish the inhibitory effect of MIF on the expression of COL1A1, COL3A1 and α-SMA and also Smad3 activation in CFs (Fig. 4C). ELISA assay results revealed that the level of pro-collagen type III amino-terminal peptide (PIIINT) was significantly lowered in the supernatant of cultured CFs treated with 12.5 or 25 ng/ml MIF protein. The levels of PIIINT and carboxyterminal propeptide of type I procollagen (PICP) were also obviously decreased in the supernatant of cultured CFs treated with 50

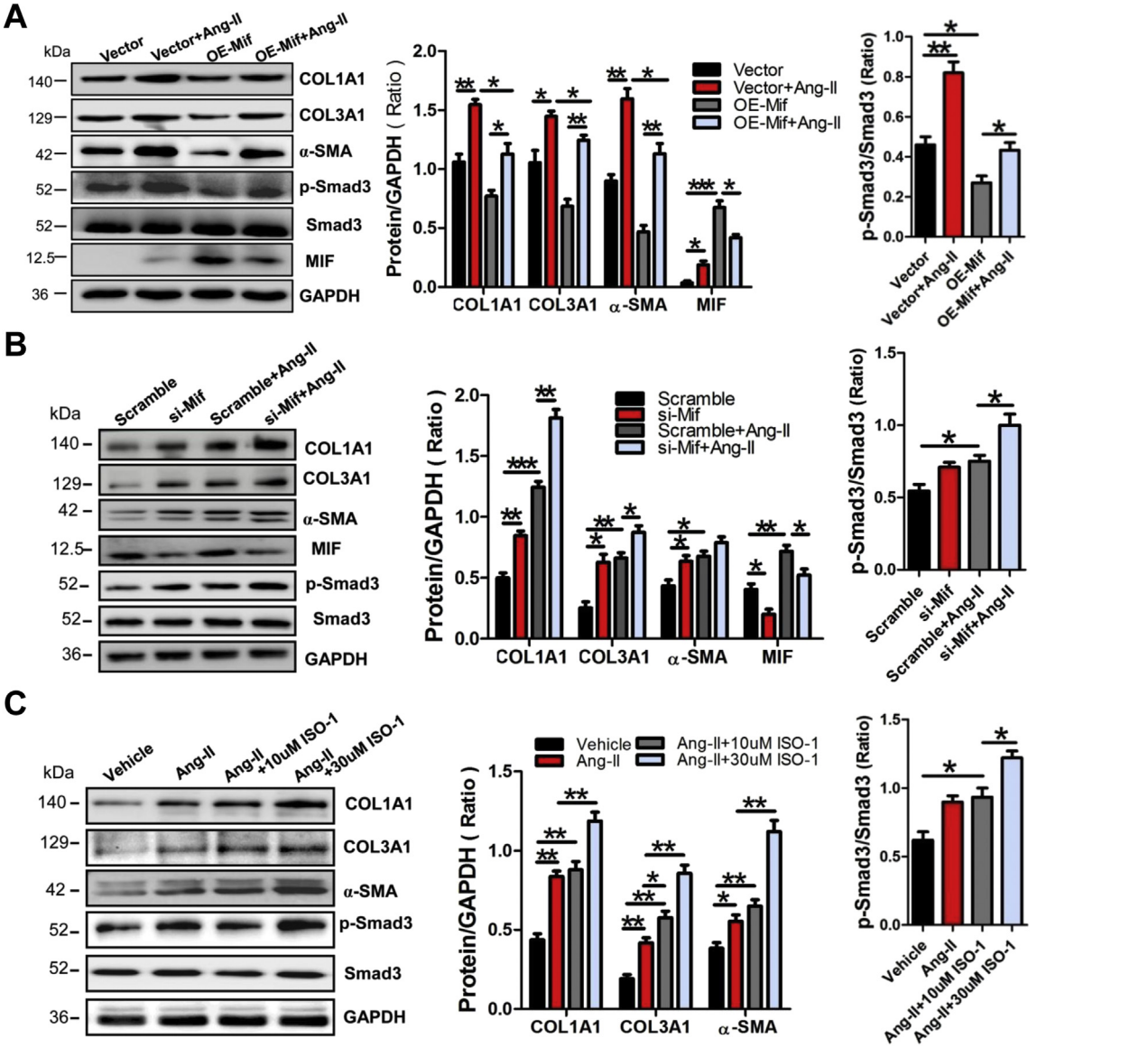

Fig. 3. Effect of MIF expression on COL1A1, COL3A1 and α-SMA expression in CFs. (A) MIF overexpression inhibited the expression of COL1A1, COL3A1 and α-SMA and smad3 activation in Ang-II-treated CFs. Data are shown as the mean ± SEM ($n = 3$). **, $P < 0.01$, ***, $P < 0.001$ vs. Vector control group. (B) MIF knockdown aggravated Ang-II-induced expression of COL1A1, COL3A1 and α-SMA, as well as Smad3 activation, in CFs. Data are shown as the mean ± SEM ($n = 3$). *, $P < 0.05$, **, $P < 0.01$, ***, $P < 0.001$. (C) MIF inhibitor ISO-1 exacerbated Ang-II-induced expression of COL1A1, COL3A1 and α-SMA, as well as Smad3 activation, in CFs. Data are shown as the mean ± SEM ($n = 3$). *, $P < 0.05$, **, $P < 0.01$.

or 75 ng/ml MIF protein, respectively (Supplementary Fig. 2A, B).

To reveal the effect of MIF on Smad3 activation, the p-Smad3 level was detected in mouse CFs at 5, 10, 30, 60 and 180 min after MIF protein treatment. Interestingly, a significant decrease in the p-Smad3 level was observed in MIF-treated CFs (Fig. 4D).

However, our data showed no significant differences in cell proliferation and cell populations in G1, S and G2/M phases in mouse CFs treated with and without MIF protein, as indicated by CCK8 assay and flow cytometry, respectively (Supplementary Fig. 3A, B). Edu assay showed that MIF overexpression had no effect on the proliferation of mouse CFs (Supplementary Fig. 3C). Additionally, trans-well migration assay demonstrated that MIF overexpression did not affect the migration of mouse CFs (Supplementary Fig. 3D).

3.5. MIF upregulates miR-29b-3p and miR-29c-3p expression in CFs

To screen the microRNAs modulated by MIF in cardiac fibrosis, microRNA profiles were analyzed in the myocardium of Ang-II-infused *Mif*-KO mice and WT control mice. MicroRNA array revealed that several microRNAs, including miR-29b-3p and miR-29c-3p, were dysregulated over 2 folds in the myocardium of *Mif*-KO mice (Fig. 5A). RT-qPCR results verified that miR-29b-3p and miR-29c-3p were significantly decreased in the myocardium of Ang-II-infused *Mif*-KO mice (Fig. 5B). We investigated the effect of MIF on miR-29b-3p and miR-29c-3p expression in mouse CFs. MiR-29b-3p and miR-29c-3p were found significantly upregulated in CFs with overexpression of MIF (Fig. 5C) and in MIF protein-treated CFs (Fig. 5D). Consistently, the precursors of miR-29b-3p and miR-29c-3p, i.e. miR-29b-1 precursor and miR-29b-2/-29c precursor (Supplementary Fig. 4A), were also found significantly down-regulated in the myocardium of Ang-II-infused *Mif*-KO mice, but markedly up-regulated in CFs with overexpression of MIF (Supplementary Fig. 4C) and in MIF protein-treated CFs (Supplementary Fig. 4D).

Fifty nM miR-29b-3p mimic or miR-29c-3p mimic was efficiently transfected into mouse CFs to investigate their effects on cardiac fibrosis (Supplementary Fig. 5). RT-qPCR and Western blot results

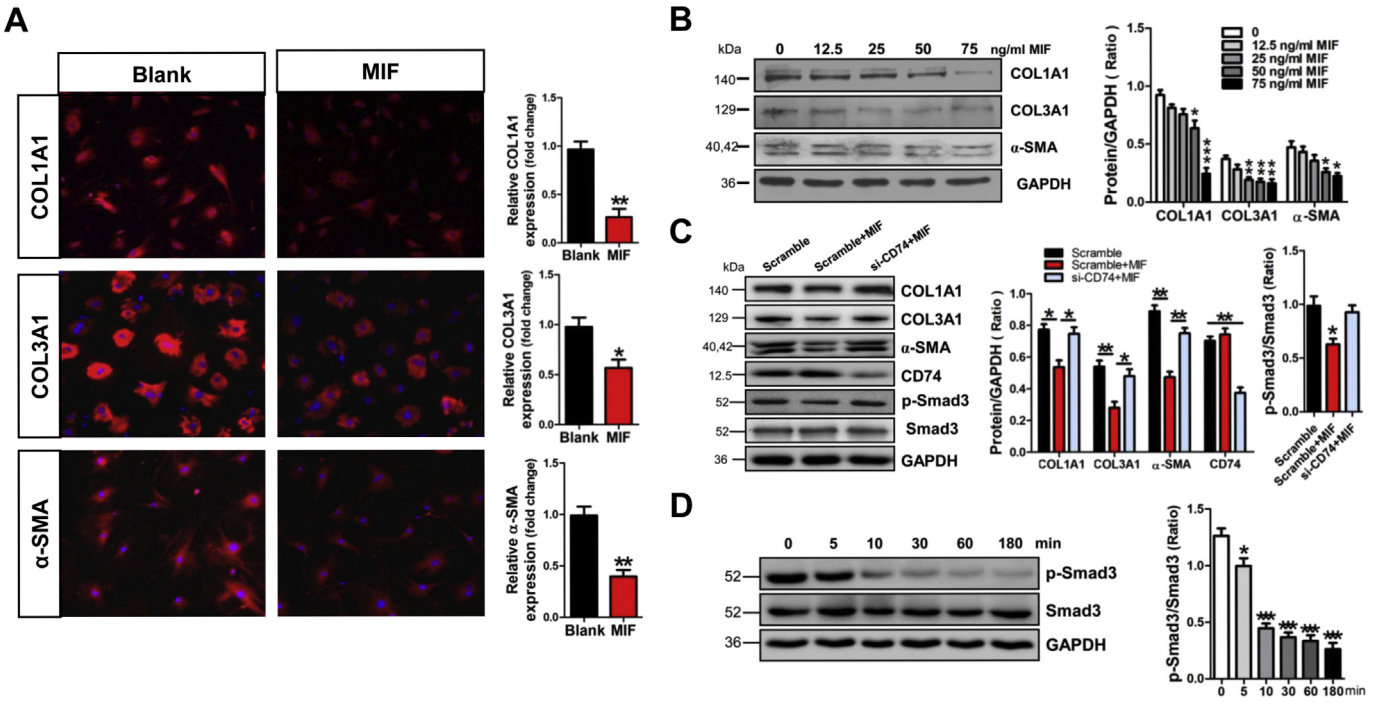

Fig. 4. MIF protein inhibits fibrosis-related gene expression in CFs. (A) MIF protein inhibited COL1A1, COL3A1 and α-SMA expression in CFs. Data are shown as the mean ± SEM ($n = 4$). (B) Protein expression of COL1A1, COL3A1, α-SMA in MIF-treated CFs as detected by Western blot assay. (C) Protein levels of COL1A1, COL3A1, α-SMA, CD74 and p-Smad3 in CFs with CD74 knockdown as detected by Western blot assay. (D) Level of p-Smad3 in MIF-treated CFs as detected by Western blot assay. Data are shown as the mean ± SEM ($n = 3$). *, $P < 0.05$, **, $P < 0.01$, ***, $P < 0.001$ vs. Blank control.

showed that mRNA and protein expression of *Col1a1, Col3a1 and Acta2* were significantly suppressed in CFs after transfection with miR-29b-3p or miR-29c-3p mimic, respectively (Fig. 5E, F). We found that 100 nM miR-29b-3p inhibitor and miR-29c-3p inhibitor could efficiently suppress MIF-upregulated miR-29b-3p and miR-29c-3p expression in CFs (Fig. 5G). Moreover, miR-29b-3p inhibitor and miR-29c-3p inhibitor could significantly attenuate the decrease of COL1A1, COL3A1 and α-SMA expression in MIF-treated CFs (Fig. 5H).

3.6. MiR-29b-3p and miR-29c-3p inhibit cardiac fibrosis by targeting Tgfb2 and Mmp2

Analysis of the databases Mirdb (www.mirdb.org) and TargetScan-Vert (www.targetscan.org) showed that *Tgfb2* and *Mmp2* were potential target genes of both miR-29b-3p and miR-29c-3p. The matching positions for miR-29b-3p and miR-29c-3p within 3′-UTRs of the targeted mRNA were shown in Fig. 6A. The dual luciferase assay demonstrated that miR-29b-3p and miR-29c-3p significantly reduced the luciferase activities through binding the sites of 2626–2632 of *Tgfb2* 3′-UTR and 258–264 of *Mmp2* 3′-UTR, respectively (Fig. 6B).

Then, we examined the expression of *Tgfb2* and *Mmp2* in CFs after transfection with miR-29b-3p and miR-29c-3p mimic, respectively. Compared with the negative scramble control, the expression of *Mmp2* mRNA, but not *Tgfb2* mRNA, and protein expression of TGF-β2 and MMP2 were significantly decreased in CFs with transfection of miR-29b-3p or miR-29c-3p mimic, respectively (Fig. 6C, D).

Next, we detected the expression of TGF-β2 and MMP2 in the myocardium of Ang-II-infused *Mif*-KO mice and WT control mice. Protein expression of TGF-β2 and MMP2 was markedly increased in the myocardium of Ang-II-infused *Mif*-KO mice (Fig. 6E), but significantly decreased in mouse CFs with overexpression of MIF (Fig. 6F).

3.7. Inactivation of Smad3 mediates MIF-upregulated expression of miR-29b-3p and miR-29c-3p

As indicated by DCFH-DA staining, Ang-II (10^{-5} M) enhanced intracellular ROS generation in mouse CFs, while 50 ng/ml MIF protein or 10 mM NAC could significantly reduce Ang-II-promoted ROS production in CFs (Fig. 7A). Western-blot results demonstrated that p-Smad3 level was elevated in Ang-II-treated CFs, but MIF or NAC treatment could efficiently abolish Ang-II-induced Smad3 activation (Fig. 7B).

RT-qPCR results showed that the expression of miR-29b-3p and miR-29c-3p was suppressed in Ang-II-treated CFs, which could be reversed by MIF or NAC treatment (Fig. 7C). Consistently, the decrease in miR-29b-1 and miR-29b-2/-29c precursors was also efficiently reversed by MIF or NAC in Ang-II-treated CFs (Supplementary Fig. 6A, B).

We further investigated the role of the Smad3 pathway in the modulation of miR-29b-3p and miR-29c-3p expression in mouse CFs. Smad3 inhibitors SIS3 and Naringenin were used to inactivate the Smad3 signaling in CFs. Our RT-qPCR results revealed that SIS3 and Naringenin could markedly reverse Ang-II-induced downregulation of miR-29b-3p and miR-29c-3p expression (Fig. 7D). Moreover, our Western blot results showed that protein expression of COL1A1, COL3A1 and α-SMA and also p-Smad3 level were significantly decreased in Ang-II-treated CFs by the pre-treatment with SIS3 or Naringenin (Supplementary Fig. 7). Additionally, *Smad3* siRNA could reverse Ang-II-downregulated expression of miR-29b-3p and miR-29c-3p in CFs (Fig. 7E).

4. Discussion

Increasing evidence suggests that MIF participates in the pathogenesis of various cardiovascular diseases [13–18]. Myocardial fibrosis in the pathological cardiac remodeling contributes to atrial fibrillation, heart failure and sudden death [2]. In the present study, we demonstrated that MIF suppresses fibrosis-associated gene expression through inactivating Smad3 and upregulating the expression of miR-29b-3p and

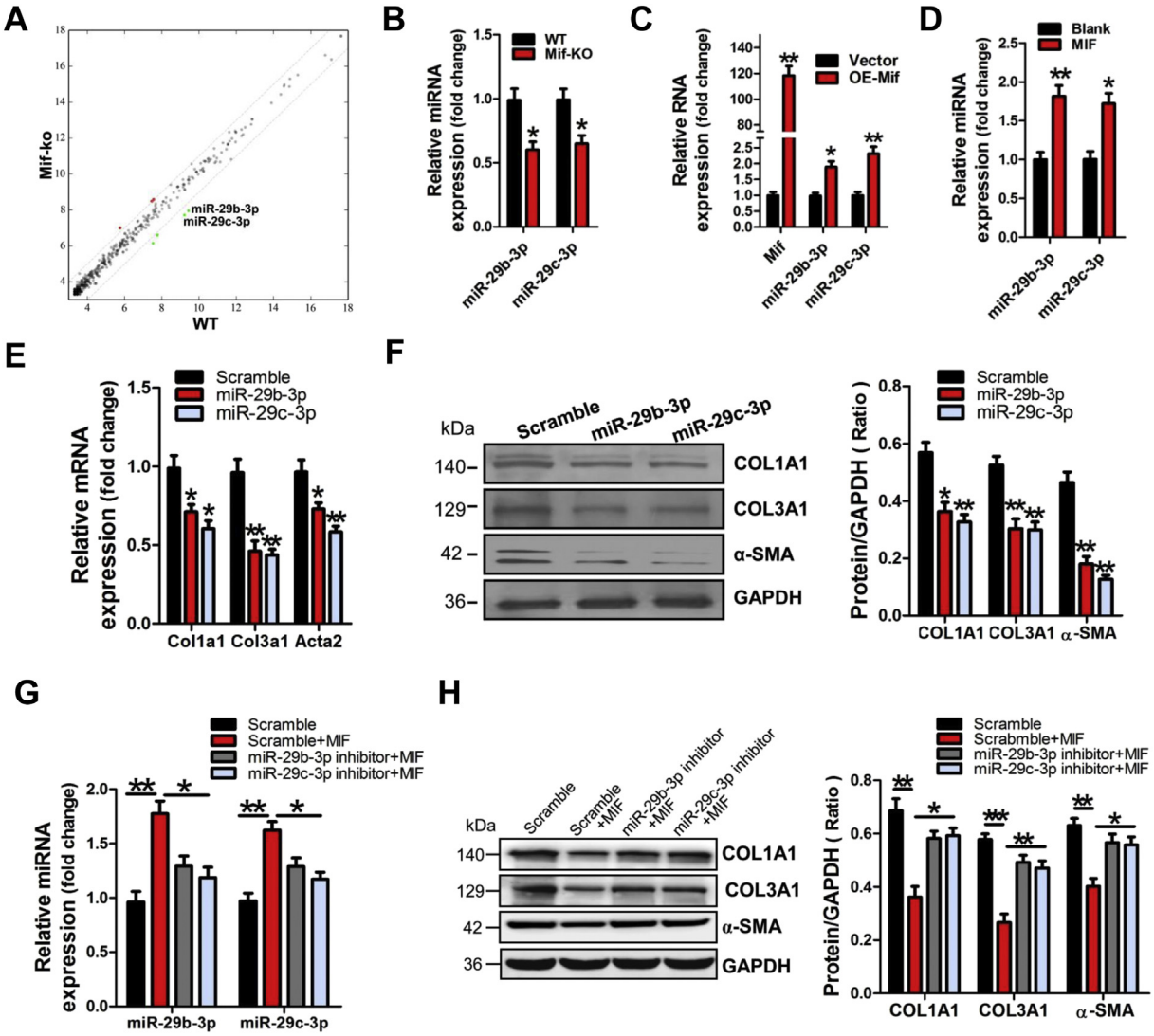

Fig. 5. MIF upregulates miR-29b-3p and -29c-3p expression in CFs. (A) The Scatter Plot figure shows the representative dysregulated microRNAs in the myocardium of Ang-II-infused *Mif*-KO mice. The values of X and Y axes in the Scatter-Plot are the normalized signal values of the samples (log2 scaled). The red dots above the top line and the green dots below the bottom line separately indicated the upregulated and downregulated miRNAs over 2.0 fold change between the two compared samples. (B) Expression of miR-29b-3p, -29c-3p was confirmed to be decreased in the myocardium of *Mif*-KO mice by RT-qPCR assay. Data are shown as the mean ± SEM ($n = 6$). *, $P < 0.05$ vs. WT mice. (C) MiR-29b-3p and miR-29c-3p were upregulated in CFs with enforced expression of MIF. Data are shown as the mean ± SEM ($n = 3$). *, $P < 0.05$, **, $P < 0.01$ vs. Vector control. (D) MiR-29b-3p and miR-29c-3p were upregulated in MIF protein-treated CFs. Data are shown as the mean ± SEM ($n = 3$). *, $P < 0.05$, **, $P < 0.01$ vs. Blank control. MiR-29b-3p and miR-29c-3p inhibited COL1A1, COL3A1 and α-SMA expression at mRNA level (E) and protein level (F) in CFs. Data are shown as the mean ± SEM ($n = 3$). *, $P < 0.05$, **, $P < 0.01$ vs. Scramble control. (G) Expression of miR-29b-3p, -29c-3p in CFs by RT-qPCR assay. (H) Expression of COL1A1, COL3A1 and α-SMA in CFs as detected by Western blot assay. Data are shown as the mean ± SEM ($n = 3$). *, $P < 0.05$, **, $P < 0.01$, ***, $P < 0.001$.

miR-29c-3p in CFs.

We observed that MIF deficiency impaired cardiac function, activated the Smad3 signaling and aggravated cardiac fibrosis in Ang-II-infused mice (Fig. 2C, D). These results were supported by the previous reports showing that knockout of MIF exacerbates hemodynamic stress-induced or aging-induced myocardial fibrosis in mice [16,19]. Moreover, our in vitro experimental data demonstrated that enforced expression of MIF (Fig. 3A) and also MIF protein (Fig. 4) could attenuate fibrosis-related gene expression and Smad3 activation in CFs. Consistently, inhibition of MIF function by *Mif* siRNA or MIF inhibitor ISO-1 could augment Ang-II-induced expression of fibrosis-related genes and Smad3 activation in CFs (Fig. 3B, C). Smad3 is considered as a crucial signaling molecule involved in tissue fibrosis [28]. Consistently, our study revealed that inactivation of Smad3 contributes to the antifibrotic effect of MIF on cardiac fibrosis. A recent report that MIF could upregulate fibrosis-related gene expression in CFs, unfortunately, the data of Smad3 activation was not provided, and Western blot results of COL1A1, COL3A1 and MMP9 were confused [29]. Moreover, the present study demonstrated that the MIF receptor, CD74 [12,30], mediates the anti-fibrotic effect of MIF in CFs (Fig. 4C).

In this study, the Smad3 signaling was found to be activated in the myocardium of Ang-II-infused *Mif*-KO mice. Accordingly, the abilities of hydroxyl radical-scavenging and superoxide anion radical-scavenging were significantly decreased in the myocardium of *Mif*-KO mice received Ang-II infusion (Supplementary Fig. 1). Our present data are consistent with the previous report that reactive oxygen species (ROS) participate in the development of fibrosis via activating the Smad3 signaling [31]. Meanwhile, the in vitro experimental results showed that MIF, also ROS inhibitor NAC, could efficiently reduce the ROS level and Smad3 activation in Ang-II-treated mouse CFs (Fig. 7). Similarly, a previous report showed that enhanced oxidative injury occurred in the hypertrophied MIF-deficient ventricle with a 10-fold increase in ROS-

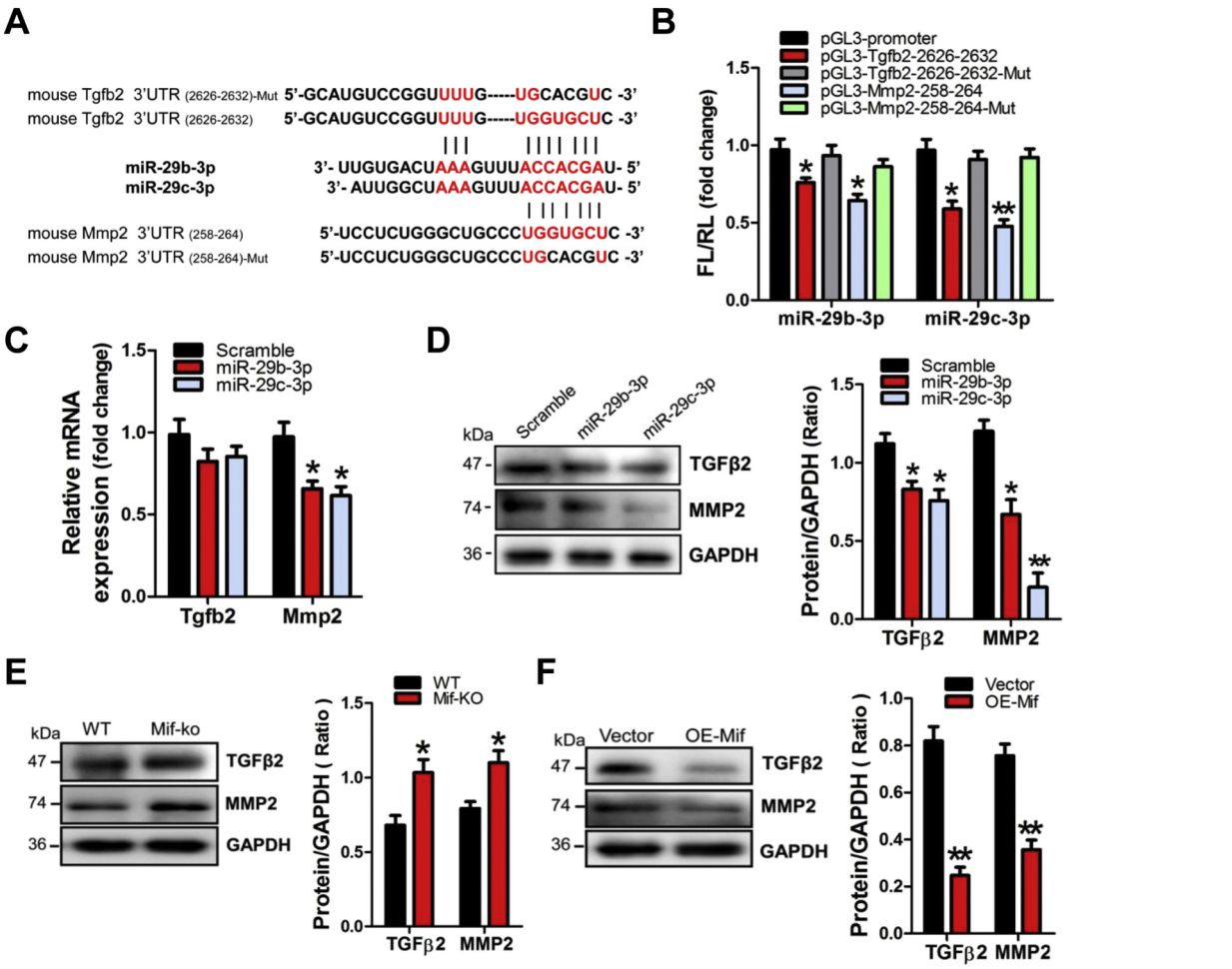

Fig. 6. Identification of *Tgfb2* and *Mmp2* as target genes of miR-29b-3p and miR-29c-3p. (A) Predicted miR-29b-3p and miR-29c-3p seed matches to the sequence in the 3′-UTRs of *Tgfb2* and *Mmp2* gene mRNA. The same seed sequence of miR-29b-3p and miR-29c-3p is AGCACCA, and the complementary nucleotide sequences are shown in red. (B) Verification of *Tgfb2* and *Mmp2* as targets of miR-29b-3p and miR-29c-3p by the dual luciferase reporter assay. Data are shown as the mean ± SEM ($n = 3$). *, $P < 0.05$, **, $P < 0.01$ vs. pGl3-promoter vector control. The mRNA (C) and protein expression (D) of *Tgfb2* and *Mmp2* in mouse CFs with and without transfection with miR-29b-3p or -29c-3p mimic, respectively. Data are shown as the mean ± SEM ($n = 3$). *, $P < 0.05$, **, $P < 0.01$ vs. Scramble control. (E) Protein expression of TGF-β2 and MMP2 in the myocardium of Ang-II-infused mice. Data are shown as the mean ± SEM ($n = 5$). *, $P < 0.05$ vs. WT mice. (F) Protein expression of TGF-β2 and MMP2 in mouse CFs. Data are shown as the mean ± SEM ($n = 3$). **, $P < 0.01$ vs. Vector control.

generating mitochondrial NADPH oxidase and a 2 to 3-fold reduction in mitochondrial SOD2 activities [16]. Moreover, a 2.3-fold increase of intracellular ROS was demonstrated in MIF-deficient cardiac fibroblasts exposed to oxidizing conditions [32].

Xue reported that MIF protein induced CF proliferation based on CCK8 assay data via an Src-dependent manner, but no further data, such as the effects of gain or loss function of Src on CFs proliferation, was provided to support this conclusion integrally [29]. In the current study, based on the experimental results of CCK8 assay, cell cycle detection, Edu assay and trans-well migration assay (Supplementary Fig. 3), we demonstrated that treatment with MIF protein or MIF overexpression had no significant effects on CF proliferation and migration. Therefore, our present study has confirmed that MIF inhibits cardiac fibrosis, but has no effects on CF proliferation and migration.

MiRNAs are known to participate in the process of cardiac fibrosis [22–24]. Among the dysregulated miRNAs in the myocardium of Ang-II-infused *Mif*-KO mice, miR-29b-3p, as well as miR-29c-3p, was found to be decreased. MiR-29b and miR-29c were known as anti-fibrotic miRNAs [33,34], but it was not clear whether they can specifically mediate the anti-fibrotic effect of MIF. The present study demonstrated that MIF specifically regulates miR-29b-3p and miR-29c-3p expression in vivo and in vitro. In parallel to mature miR-29b-3p and miR-29c-3p, miR-29b-1 and miR-29b-2/-29c precursors were also confirmed to be decreased in the myocardium of Ang-II-infused *Mif*-KO mice, but increased in mouse CFs in response to enforced expression of MIF and treatment with MIF protein, respectively. These above results indicate that MIF enhances the expressions of miR-29b-3p and miR-29c-3p at the transcriptional level.

In agreement with previous reports [33,34], we confirmed that miR-29b-3p and miR-29c-3p possess the same seed sequence (AGCACCA) and inhibit *Col1a1* and *Col3a1* expression at the transcriptional level. Importantly, *Tgfb2* and *Mmp2*, two known pro-fibrosis genes in organ fibrosis [35], were identified as novel targets genes of miR-29b-3p and miR-29c-3p in the present study. MiR-29b-3p and miR-29c-3p could suppress *Tgfb2* and *Mmp2* expression at the post-transcriptional and transcriptional levels, respectively. In parallel to COL1A1, COL3A1, TGF-β2 and MMP2 were also shown to be consistently increased in the myocardium of Ang-II-infused *Mif*-KO mice, but markedly decreased in mouse CFs with enforced expression of MIF. Therefore, the present study has demonstrated that miR-29b-3p and miR-29c-3p mediate the anti-fibrotic effect of MIF through targeting *Tgfb2* and *Mmp2* in CFs.

Meanwhile, the present study has shown that Smad3 activation was negatively correlated with miR-29b-3p and miR-29c-3p expression in vivo (Figs. 2D, 5A, B, Supplementary Fig. 4B) and in vitro (Figs. 3A, 4C, 5C, D, Supplementary Fig. 4C, D), and both MIF and NAC could attenuate Ang-II-induced Smad3 activation, resulting in upregulation of

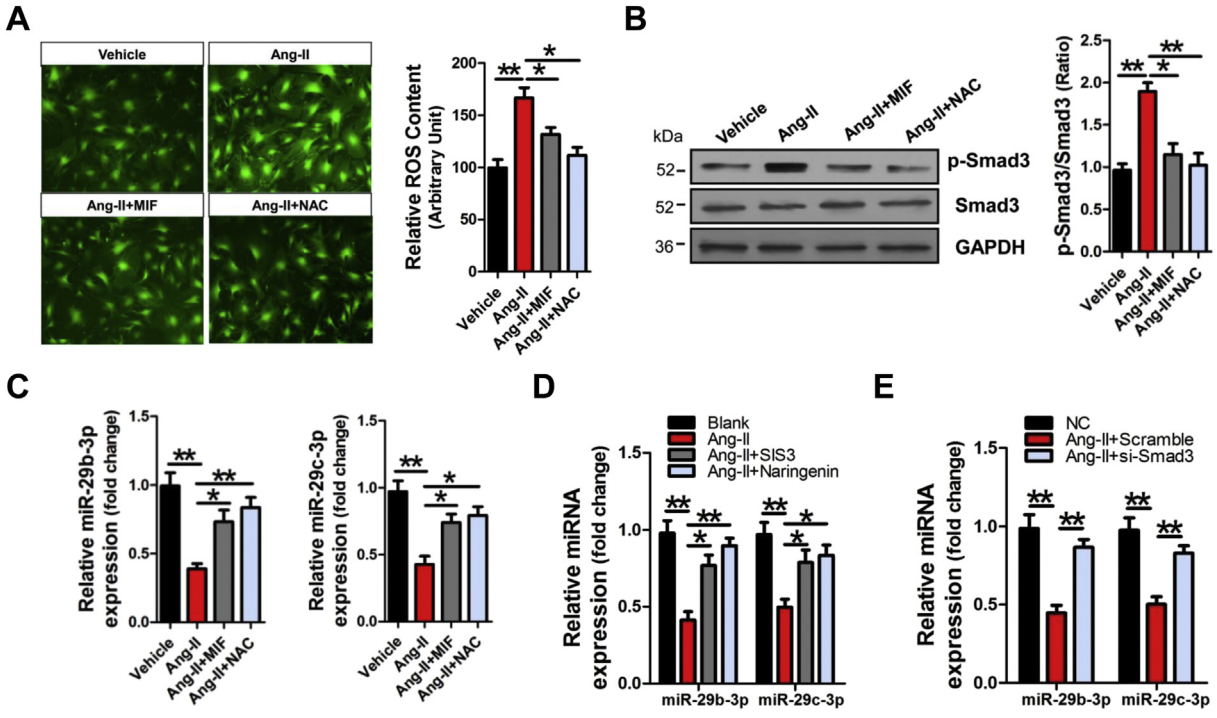

Fig. 7. MIF upregulates the expression of miR-29b-3p and miR-29c-3p through inactivating the Smad3 signaling. (A) MIF inhibited Ang-II-promoted ROS generation in mouse CFs. (B) Detection of p-Smad3 level in mouse CFs. (C) MIF reversed Ang-II-downregulated expression of miR-29b-3p and miR-29c-3p in mouse CFs. Smad3 inhibitors SIS-3 and Naringenin (D) and *Smad3* siRNA (E) reversed Ang-II-downregulated expression of miR-29b-3p and miR-29c-3p in mouse CFs. Data are shown as the mean ± SEM ($n = 3$). *, $P < 0.05$, **, $P < 0.01$.

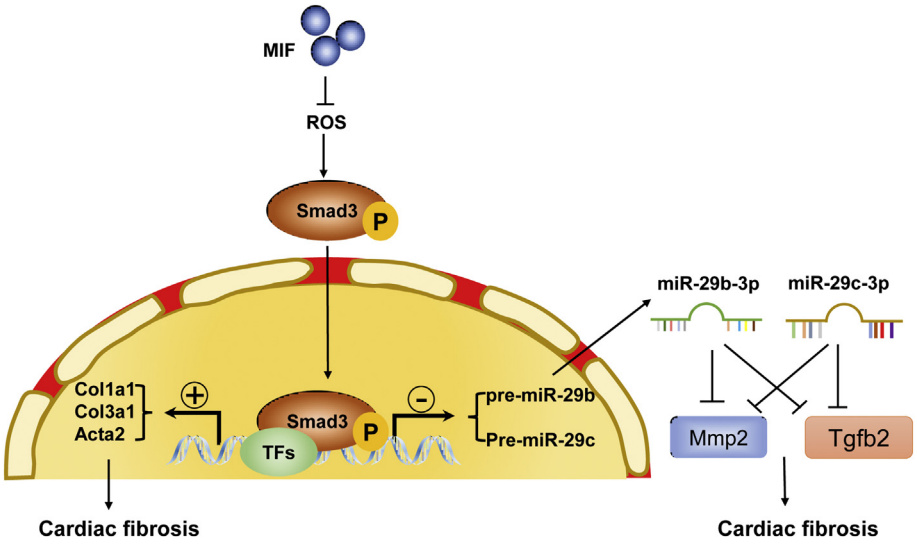

Fig. 8. Schematic diagram of the mechanism whereby MIF attenuates cardiac fibrosis. Inactivation of the Smad3 signaling by MIF contributes to attenuation of fibrosis-related gene expression in CFs. Meanwhile, upregulation of miR-29b-3p and miR-29c-3p by Smad3 inactivation also contributes to the suppression of cardiac fibrosis by targeting *Tgfb2* and *Mmp2* in CFs.

the expression of miR-29b-3p and miR-29c-3p in mouse CFs (Fig. 7B, C, Supplementary Fig. 5). We further verified that blocking Smad3 activation by Smad3 inhibitors SIS-3 and Naringenin and *Smad3* siRNA could consistently reverse Ang-II-induced downregulation of miR-29b-3p and miR-29c-3p expression in mouse CFs (Fig. 7D, E). These results were supported by previous reports that the Smad3 signaling promotes fibrosis by inhibiting miR-29 expression [36,37]. Therefore, our data demonstrated that inactivation of Smad3 mediates MIF-upregulated expression of miR-29b-3p and miR-29c-3p in mouse CFs. However, the underlying mechanism that Smad3 negatively modulates miR-29b-3p and miR-29c-3p expression warrants further investigation.

Taken together, our results have demonstrated that MIF expression was up-regulated in mouse fibrotic myocardium and Ang-II-treated CFs. MIF could suppress the expression of fibrosis-related genes, but without any effect on CF proliferation and migration. MIF could attenuate ROS levels, suppress Smad3 activation and up-regulate the expression of miR-29b-3p and miR-29c-3p, which inhibit cardiac fibrosis through targeting *Tgfb2* and *Mmp2* in CFs. Therefore, the present study suggests that MIF suppresses cardiac fibrosis through regulating the Smad3-miR-29b/miR-29c axis, as illustrated in Fig. 8.

Transparency document

The Transparency document associated with this article can be found, in online version.

Acknowledgement

This study was supported by the following grants: National Science Foundation of China, China (91649109, 81470439, 81770264); Guangzhou Science and Technology Program key projects, China (201804010045), and High-level Hospital Construction Project of Guangdong General Hospital, China (DFJH201807).

Declaration of Competing Interest

All authors have no conflict of interest.

Appendix A. Supplementary data

Supplementary data to this article can be found online at https://doi.org/10.1016/j.bbadis.2019.06.004.

References

[1] B.C. Berk, K. Fujiwara, S. Lehoux, ECM remodeling in hypertensive heart disease, J. Clin. Invest. 117 (2007) 568–575.
[2] Z. Fan, J. Guan, Antifibrotic therapies to control cardiac fibrosis, Biomater Res 20 (2016) 13.
[3] R. Kleemann, A. Kapurniotu, R.W. Frank, A. Gessner, R. Mischke, O. Flieger, S. Jüttner, H. Brunner, J. Bernhagen, Disulfide analysis reveals a role for macrophage migration inhibitory factor (MIF) as thiol-protein oxidoreductase, J. Mol. Biol. 280 (1998) 85–102.
[4] R. Kleemann, R. Mischke, A. Kapurniotu, H. Brunner, J. Bernhagen, Specific reduction of insulin disulfides by macrophage migration inhibitory factor (MIF) with glutathione and dihydrolipoamide: potential role in cellular redox processes, FEBS Lett. 430 (1998) 191–196.
[5] T. Calandra, B. Echtenacher, D.L. Roy, J. Pugin, C.N. Metz, L. Hültner, D. Heumann, D. Männel, R. Bucala, M.P. Glauser, Protection from septic shock by neutralization of macrophage migration inhibitory factor, Nat. Med. 6 (2000) 164–170.
[6] J.A. Baugh, S. Chitnis, S.C. Donnelly, J. Monteiro, X. Lin, B.J. Plant, F. Wolfe, P.K. Gregersen, R. Bucala, A functional promoter polymorphism in the macrophage migration inhibitory factor (MIF) gene associated with disease severity in rheumatoid arthritis, Genes Immun. 3 (2002) 170–176.
[7] E.F. Morand, M. Leech, J. Bernhagen, MIF: a new cytokine link between rheumatoid arthritis and atherosclerosis, Nat. Rev. Drug Discov. 5 (2006) 399–410.
[8] L. Verschuren, T. Kooistra, J. Bernhagen, P.J. Voshol, D.M. Ouwens, M. van Erk, J. de Vries-van der Weij, L. Leng, J.H. van Bockel, K.W. van Dijk, G. Fingerle-Rowson, R. Bucala, R. Kleemann, MIF deficiency reduces chronic inflammation in white adipose tissue and impairs the development of insulin resistance, glucose intolerance, and associated atherosclerotic disease, Circ. Res. 105 (2009) 99–107.
[9] S.G. Lin, X.Y. Yu, Y.X. Chen, X.R. Huang, C. Metz, R. Bucala, C.P. Lau, H.Y. Lan, De novo expression of macrophage migration inhibitory factor in atherogenesis in rabbits, Circ. Res. 87 (2000) 1202–1208.
[10] A. Zernecke, J. Bernhagen, C. Weber, Macrophage migration inhibitory factor in cardiovascular disease, Circulation 117 (2008) 1594–1602.
[11] C. Tong, A. Morrison, X. Yan, P. Zhao, E.D. Yeung, J. Wang, J. Xie, J. Li, Macrophage migration inhibitory factor deficiency augments cardiac dysfunction in type 1 diabetic murine cardiomyocytes, J Diabetes 2 (2010) 267–274.
[12] Y. Liang, W. Yuan, W. Zhu, J. Zhu, Q. Lin, X. Zou, C. Deng, Y. Fu, X. Zheng, M. Yang, S. Wu, X. Yu, Z. Shan, Macrophage migration inhibitory factor promotes expression of GLUT4 glucose transporter through MEF2 and Zac1 in cardiomyocytes, Metabolism 64 (2015) 1682–1693.
[13] D.A. White, Y. Su, P. Kanellakis, H. Kiriazis, E.F. Morand, R. Bucala, A.M. Dart, X.M. Gao, X.J. Du, Differential roles of cardiac and leukocyte derived macrophage migration inhibitory factor in inflammatory responses and cardiac remodelling post myocardial infarction, J. Mol. Cell. Cardiol. 69 (2014) 32–42.
[14] E.J. Miller, J. Li, L. Leng, C. McDonald, T. Atsumi, R. Bucala, L.H. Young, Macrophage migration inhibitory factor stimulates AMP-activated protein kinase in the ischaemic heart, Nature 451 (2008) 578–582.
[15] H. Ma, J. Wang, D.P. Thomas, C. Tong, L. Leng, W. Wang, M. Merk, S. Zierow, J. Bernhagen, J. Ren, R. Bucala, J. Li, Impaired macrophage migration inhibitory factor-AMP-activated protein kinase activation and ischemic recovery in the senescent heart, Circulation 122 (2010) 282–292.
[16] K. Koga, A. Kenessey, K. Ojamaa, Macrophage migration inhibitory factor antagonizes pressure overload-induced cardiac hypertrophy, Am. J. Physiol. Heart Circ. Physiol. 304 (2013) H282–H293.
[17] X. Xu, Y. Hua, S. Nair, R. Bucala, J. Ren, Macrophage migration inhibitory factor deletion exacerbates pressure overload-induced cardiac hypertrophy through mitigating autophagy, Hypertension 63 (2014) 490–499.
[18] X. Xu, B.D. Pacheco, L. Leng, R. Bucala, J. Ren, Macrophage migration inhibitory factor plays a permissive role in the maintenance of cardiac contractile function under starvation through regulation of autophagy, Cardiovasc. Res. 99 (2013) 412–421.
[19] X. Xu, J. Pang, Y. Chen, R. Bucala, Y. Zhang, J. Ren, Macrophage migration inhibitory factor (MIF) deficiency exacerbates aging-induced cardiac remodeling and dysfunction despite improved inflammation: role of autophagy regulation, Sci. Rep. 6 (2016) 22488.
[20] E. van Rooij, E.N. Olson, Searching for miR-acles in cardiac fibrosis, Circ. Res. 104 (2009) 138–140.
[21] G. Condorelli, M.V. Latronico, G.W.I.I. Dorn, MicroRNAs in heart disease: putative novel therapeutic targets, Eur. Heart J. 31 (2010) 649–658.
[22] J. Bauersachs, Regulation of myocardial fibrosis by microRNAs, J. Cardiovasc. Pharmacol. 56 (2010) 454–459.
[23] W.S. Zhu, C.M. Tang, Z. Xiao, J.N. Zhu, Q.X. Lin, Y.H. Fu, Z.Q. Hu, Z. Zhang, M. Yang, X.L. Zheng, S.L. Wu, Z.X. Shan, Targeting EZH1 and EZH2 contributes to the suppression of fibrosis-associated genes by miR-214-3p in cardiac myofibroblasts, Oncotarget 7 (2016) 78331–78342.
[24] L. Tao, Y. Bei, P. Chen, Z. Lei, S. Fu, H. Zhang, J. Xu, L. Che, X. Chen, J.P. Sluijter, S. Das, D. Cretoiu, B. Xu, J. Zhong, J. Xiao, X. Li, Crucial role of miR-433 in regulating cardiac fibrosis, Theranostics 6 (2016) 2068–2083.
[25] C.M. Tang, F.Z. Liu, J.N. Zhu, Y.H. Fu, Q.X. Lin, C.Y. Deng, Z.Q. Hu, H. Yang, X.L. Zheng, J.D. Cheng, S.L. Wu, Z.X. Shan, Myocyte-specific enhancer factor 2C: a novel target gene of miR-214-3p in suppressing angiotensin II-induced cardiomyocyte hypertrophy, Sci. Rep. 6 (2016) 36146.
[26] Y. Liang, Q. Lin, J. Zhu, X. Li, Y. Fu, X. Zou, X. Liu, H. Tan, C. Deng, X. Yu, Z. Shan, W. Yuan, The caspase-8 shRNA-modified mesenchymal stem cells improve the function of infarcted heart, Mol. Cell. Biochem. 397 (2014) 7–16.
[27] W. Yuan, C. Tang, W. Zhu, J. Zhu, Q. Lin, Y. Fu, C. Deng, Y. Xue, M. Yang, S. Wu, Z. Shan, CDK6 mediates the effect of attenuation of miR-1 on provoking cardiomyocyte hypertrophy, Mol. Cell. Biochem. 412 (2016) 289–296.
[28] H.H. Hu, D.Q. Chen, Y.N. Wang, Y.L. Feng, G. Cao, N.D. Vaziri, Y.Y. Zhao, New insights into TGF-β/Smad signaling in tissue fibrosis, Chem. Biol. Interact. 292 (2018) 76–83.
[29] Y.M. Xue, C.Y. Deng, W. Wei, F.Z. Liu, H. Yang, Y. Liu, X. Li, Z. Wang, S.J. Kuang, S.L. Wu, F. Rao, Macrophage migration inhibitory factor promotes cardiac fibroblast proliferation through the Src kinase signaling pathway, Mol. Med. Rep. 17 (2018) 3425–3431.
[30] L. Leng, C.N. Metz, Y. Fang, J. Xu, S. Donnelly, J. Baugh, T. Delohery, Y. Chen, R.A. Mitchell, R. Bucala, MIF signal transduction initiated by binding to CD74, J. Exp. Med. 197 (2003) 1467–1476.
[31] F. Gao, V.L. Kinnula, M. Myllärniemi, T.D. Oury, Extracellular superoxide dismutase in pulmonary fibrosis, Antioxid. Redox Signal. 10 (2008) 343–354.
[32] K. Koga, A. Kenessey, S.R. Powell, C.P. Sison, E.J. Miller, K. Ojamaa, Macrophage migration inhibitory factor provides cardioprotection during ischemia/reperfusion by reducing oxidative stress, Antioxid. Redox Signal. 14 (2011) 1191–1202.
[33] J.N. Zhu, R. Chen, Y.H. Fu, Q.X. Lin, S. Huang, L.L. Guo, M.Z. Zhang, C.Y. Deng, X. Zou, S.L. Zhong, M. Yang, J. Zhuang, X.Y. Yu, Z.X. Shan, Smad3 inactivation and miR-29b upregulation mediate the effect of carvedilol on attenuating the acute myocardium infarction-induced myocardial fibrosis in rat, PLoS One 8 (2013) e75557.
[34] L. Liu, B. Ning, J. Cui, T. Zhang, Y. Chen, miR-29c is implicated in the cardioprotective activity of Panax notoginseng saponins against isoproterenol-induced myocardial fibrogenesis, J. Ethnopharmacol. 198 (2017) 1–4.
[35] J.A. Eldred, L.M. Hodgkinson, L.J. Dawes, J.R. Reddan, D.R. Edwards, I.M. Wormstone, MMP2 activity is critical for TGFβ2-induced matrix contraction–implications for fibrosis, Invest. Ophthalmol. Vis. Sci. 53 (2012) 4085–4098.
[36] J. Xiao, X.M. Meng, X.R. Huang, A.C. Chung, Y.L. Feng, D.S. Hui, C.M. Yu, J.J. Sung, H.Y. Lan, miR-29 inhibits bleomycin-induced pulmonary fibrosis in mice, Mol. Ther. 20 (2012) 1251–1260.
[37] W. Qin, A.C. Chung, X.R. Huang, X.M. Meng, D.S. Hui, C.M. Yu, J.J. Sung, H.Y. Lan, TGF-β/Smad3 signaling promotes renal fibrosis by inhibiting miR-29, J. Am. Soc. Nephrol. 22 (2011) 1462–1474.